Advances in Non-Stationary Frequency Modulated Thermal Wave Imaging for Non-Destructive Testing and Evaluation

by G. Dua and R. Mulaveesala*

InfraRed Imaging Laboratory, Indian Institute of Technology Ropar, Punjab, *ravibabucareiitd@yahoo.co.in

Abstract

Among the widely used Non-Destructive Testing and evaluation approaches, InfraRed Thermography has proven to be one of the vital NDT technique due to its inherent capabilities for testing and evaluation of various solid materials. Nevertheless, there are some limitations; depending upon the test approach used, as well as the adopted data processing method. In active approach of infrared thermography, most widely used excitation sources are optical excitation due to its wide area remote heating capabilities with the intention of heat flow into the test specimen. The temperature differences during transient heating over the material is used for subsurface defects detection. Since the heating features of the stimulus sources are well known (duration and it's amplitude level), they can be considered for quantitative information. However, when a material is heated, the thermal waves penetrate into the material. The waves generally of various amplitudes for chosen band of frequencies or a mono frequency sinusoidal thermal excitation are launched into the specimen during the active heating. This work presents a transient non-stationary thermographic testing technique (which can utilize desired band of frequencies in limited span of time), concerning the assessment of metallic material with artificial defects introduced.

1. Introduction (Arial, 9pt, bold)

Thermal Wave Imaging (TWI) is a two-dimensional, remote, non-contact technique of mapping surface temperature distribution which can be properly utilized for Non-Destructive Testing and Evaluation (NDT&E) [1] of materials. Prominent advances and recent studies indicate that TWI can be used in remote characterization of different materials [2-11]. The objective of TWI is to capture transient thermal images of the test specimen under inspection by providing heat energy to generate thermal waves within the specimen. The experiments involve imaging surface and subsurface structures with industrial and medical applications, as well as the quantitative characterization of the thermal properties of materials. This paper focuses on the inspection of mild steel material, which is extensively used in various industries like construction, transportation, oil and gas etc. Most commonly used industrial components made up of mild steel include construction beams, chimneys, sliding and rod type gates etc. Safety and demand for quality of in-service products, require thorough testing and reliable monitoring methodology to avoid risky failures. The characterization of materials and of the processes going on in them is of considerable interest for the design of components in order to operate them in a safe and reliable way. Non-stationary thermal-wave imaging methodology has been signifying as a consistent material characterization capabilities in thermographic NDT&E [12-30]. These techniques aid the use of low peak power heat sources in a moderate time compared with the conventionally used pulsed thermography (PT) [5], pulse phase thermography (PPT) [3] and sinusoidal modulated (lock-in) thermography [7,8] technique. For many applications, the technique has proven to be a cost effective alternative to traditional inspection technologies. This paper highlights the capability of Frequency Modulated Thermal Wave Imaging (FMTWI) [12-15] technique in visualizing inclusions present in modeled mild steel sample. In FMTWI the incident heat flux is varied by driving the heat sources with a linear frequency modulated signal (in up chirp form), which causes a similar frequency modulated surface heating over the sample. This helps to introduce desired band of frequencies with significant magnitude into the test sample which improves the test resolution. Further, different transform techniques [25,30] have been implemented on the resulting captured temperature distribution and compared by taking Signal to Noise Ratio (SNR) into consideration.

2. Modelling and Simulation

In this presented work, a 3-Dimensional (3D) Finite Element Analysis (FEA) has been carried out on a mild steel sample using COMSOL Multiphysics. The mild steel sample with six inclusions {Air, Calcium Fluoride (CaF_2), Calcium Oxide (CaO), Titanium Oxide (TiO_2), Aluminium Oxide (Al_2O_3) and Magnesium Oxide (MgO)} has been modeled with a finer mesh using 3D tetrahedral elements. The modeled sample is as shown in figure 1. The sample is having dimensions of 150×50×6 (in millimeters). Each inclusion is intentionally kept as an ellipsoid with a-semiaxis:10, b-semiaxis:4, c-semiaxis:2 at a depth of 1 mm from the front surface. The basic properties of mild steel and the introduced inclusions are as given in table 1. The FEA was carried out by imposing a LFM heat flux over the surface of the test object and the corresponding surface thermal response has been obtained. The simulations were carried out under adiabatic boundary conditions, with the sample at an ambient temperature of 300 K.
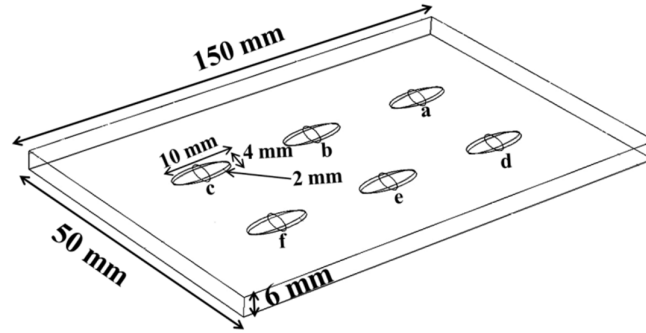
Fig. 1. *Layout of the modeled mild steel sample with inclusions*

Table 1. *Sample Properties*

Thermal Property	Material						
	Air	CaF$_2$	CaO	TiO$_2$	Al$_2$O$_3$	MgO	Mild steel
Density (Kg/m^3)	1.225	3180	3350	4250	3975	3580	7850
Thermal Conductivity (W/m-K)	0.024	9.71	15	13	30.3	36	60.5
Specific Heat (J/Kg-K)	1010	854	749	711.28	880	960	434

3. Data Analysis

3.1. Frequency Domain Analysis

Suppose $s(n)$ is a temporal temperature data captured at a predefined rate obtained for a given pixel (i,j) in the field of view, then its Fourier transform $S(f)$ is given as [3]:

$$S(f) = \frac{1}{N}\sum_{n=0}^{N-1} s(n)exp\left(\frac{-j2\pi fn}{N}\right) = Real(f) + Imag(f) \tag{1}$$

where $Real(f)$ and $Imag(f)$ are the real and imaginary components of $S(f)$ respectively.
Further, the phase can be computed as follows [3]:

$$\varphi(f) = tan^{-1}\left(\frac{Imag(f)}{Real(f)}\right) \tag{2}$$

3. 2. Time Domain Analysis

The time domain correlation coefficient (CC) image is computed from the circular convolution between the chosen reference signal with the captured temperature response given as follows [29,30]

$$CC(\tau) = \mathfrak{I}^{-1}\{Ref(f)^* . S(f)\} \tag{3}$$

where $Ref(f)$ and $S(f)$ are the Fourier transforms of the reference temperature signal $ref(t)$ and the captured temperature response $s(t)$, $\mathfrak{I}^{-1}$ and $*$ denote the inverse Fourier transform and complex conjugate operators, respectively. In time domain analysis, the role of linear FMTWI is to compress the energy delivered by the frequency modulated heat flux into a narrow correlation peak which enables imaging with high depth resolution. The result is a reduction in the width of the main lobe and an increase in the amplitude of the CC peak as the supplied energy needs to be unaltered. However, time domain phase image is constructed from the circular convolution of the in-phase as well as quadrature-phase of the chosen reference signal with that of the captured temperature response. It is given as [29,30]

$$\varphi(\tau) = cot^{-1}\left\{\frac{\mathfrak{I}^{-1}\{Ref(f)^* S(f)\}}{\mathfrak{I}^{-1}\{[-isgn(f)Ref(f)]^* S(f)\}}\right\} \tag{4}$$

where $sgn(f)$ is the signum function. The expression inside the squared bracket is the frequency response of the quadrature reference signal. The quadrature of the reference temperature response is obtained using Hilbert Transform

(HT) and the frequency response is obtained through Discrete Fourier Transform (DFT). The process is explained using a block diagram shown in figure 2.
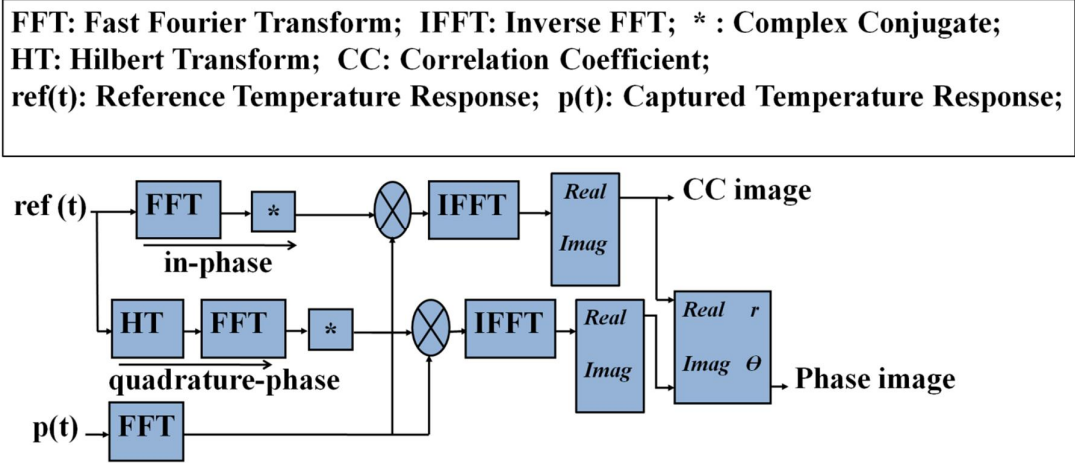
FFT: Fast Fourier Transform; IFFT: Inverse FFT; * : Complex Conjugate; HT: Hilbert Transform; CC: Correlation Coefficient; ref(t): Reference Temperature Response; p(t): Captured Temperature Response;

Fig. 2. *The processing approach adopted for construction of time domain correlation co-efficient and phase contrast images [29,30].*

4. Results and Discussion

The modeled mild steel sample with inclusions is simulated using controlled frequency modulated heat flux with frequency sweeping from 0.01Hz to 0.1Hz in 100 s. The resulting temporal temperature response is obtained and further processed by applying different data analysis techniques as mentioned above. Results so obtained are shown in figure.3 The conventional frequency domain image is shown in figure. 3 (a), whereas the time domain phase image is shown in figure. 3 (b). The time domain correlation coefficient image is shown in figure.3 (c). It clearly indicates that materials with different thermal properties gives different thermal contrast, therefore can be easily utilized for identification of sub-surface feature characteristic and its properties. Further, Thermal contrasts have been quantified in terms of the materials Signal to Noise Ratio (SNR) computed using:

$$SNR = 20\log\left(\frac{Mean\ of\ the\ inclusion\ region - Mean\ of\ the\ mild\ steel\ region}{Standard\ deviation\ of\ mild\ steel\ region}\right) \tag{5}$$

SNRs have been computed for different inclusions in the mild steel sample for the data processed with different analysis techniques. The value of SNRs are as given in table 2.
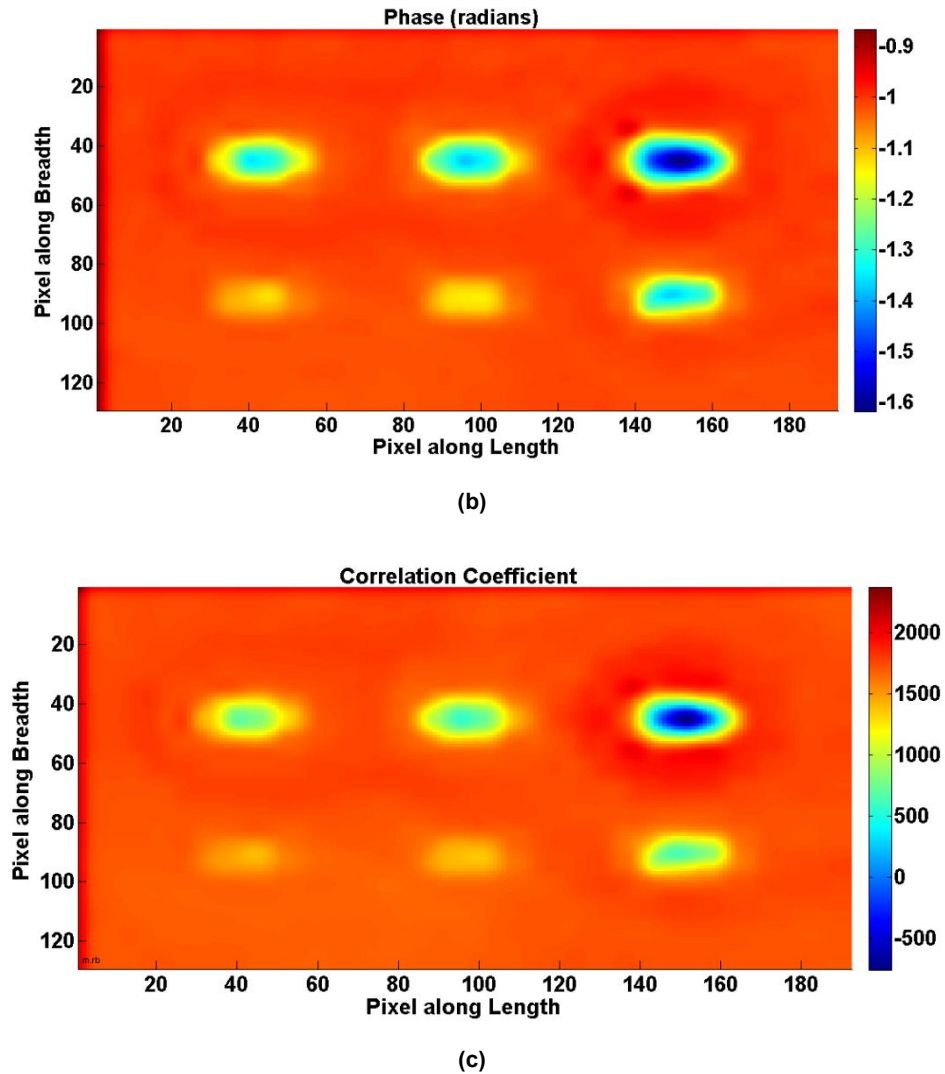

(a)

(b)

(c)
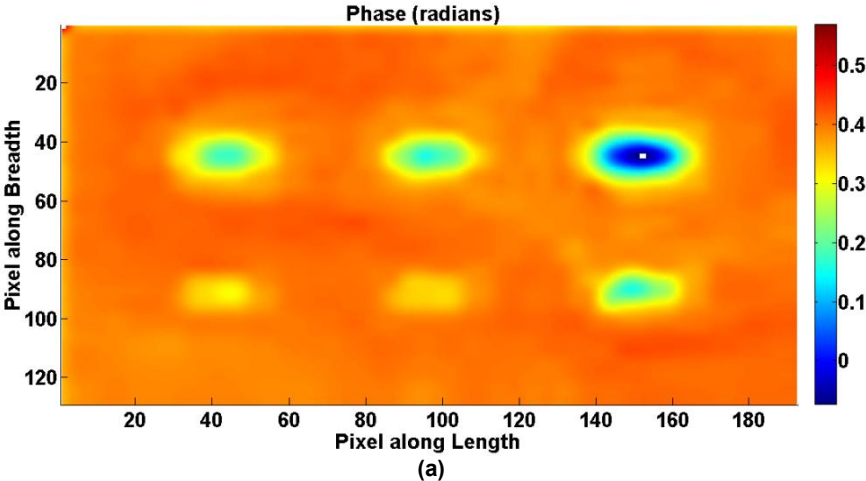
Fig. 3. *Results obtained for frequency and time domain transform techniques. (a). frequency domain phase image. (b). time domain phase image. (c). time domain correlation coefficient image.*

Table 2. *Signal to Noise Ratio*

Transform Technique	SNR in Decibels (dB) for different inclusions					
	Air (a)	CaF$_2$ (b)	CaO (c)	TiO$_2$ (d)	Al$_2$O$_3$ (e)	MgO (f)
FFT Phase	91.2794	81.8481	77.9304	76.7255	47.8721	47.6980
Time Domain Phase	136.8374	128.5947	126.8325	126.0722	96.4528	89.7353
Time Domain Correlation	115.3984	104.4740	99.4589	98.8497	67.7099	64.1536

REFERENCES

[1] Maldague, X. P. V., Theory and Practice of Infrared Thermography for Nondestructive Testing, New York: Wiley (2001).

[2] Sakagami, T. and Kubo, S., "Applications of pulse heating thermography and lock-in thermography to quantitative nondestructive evaluations," Infrared Physics and Technology, 43(3-5), 211-218 (2002).

[3] Maldague, X. and Marinetti, S., "Pulse phase infrared thermography," Journal of Applied Physics, 79(5), 2694-2698 (1996).

[4] Avdelidis, N. P., Almond, D. P., Dobbinson, A., Hawtin, B. C., Ibarra-Castanedo, C. and Maldague, X. P. V., "Aircraft composites assessment by means of transient thermal NDT," Progress in Aerospace Sciences, 40(3), 143-162 (2004).

[5] Almond, D. P. and Lau, S. K., "Defect sizing by transient thermography. I: An analytical treatment," Journal of Physics D: Applied Physics, 27(5), 1063-1069 (1994).

[6] Rosencwaig, A., "Thermal-wave imaging," Science, 218(4569), 223-228 (1982).

[7] Busse, G., and Eyerer, P., "Thermal wave remote and nondestructive inspection of polymers," Applied Physics Letters, 43(4), 355-357. doi: 10.1063/1.94335 (1983).

[8] Busse, G., Wu, D. and Karpen, W., "Thermal wave imaging with phase sensitive modulated thermography," Journal of Applied Physics, 71(8), 3962-3965 (1992).

[9] Meola, C., Carlomagno, G. M., Squillace, A., and Giorleo, G., "Non-destructive control of industrial materials by means of lock-in thermography," Measurement Science and Technology, 13(10), 1583-1590 (2002).

[10] Dillenz, A., Zweschper, T., Riegert, G., and Busse, G., "Progress in phase angle thermography," Review of Scientific Instruments, 74(1 II), 417-419 (2003).

[11] Peng, D. and Jones, R., "Modelling of the lock-in thermography process through finite element method for estimating the rail squat defects," Engineering Failure Analysis, 28, 275-288 (2013).

[12] Mulaveesala, R. and Tuli, S., "Digitized frequency modulated thermal wave imaging for nondestructive testing," Materials Evaluation, 63(10), 1046-1050 (2005).

[13] Mulaveesala, R. and Tuli, S., "Theory of frequency modulated thermal wave imaging for nondestructive subsurface defect detection," Applied Physics Letters, 89(19), 191913 (2006).

[14] Mulaveesala, R., Vaddi, J. S. and Singh, P., "Pulse compression approach to infrared nondestructive characterization," Review of Scientific Instruments, 79(9), 094901 (2008).

[15] Ghali, V. S., Jonnalagadda, N. and Mulaveesala, R., "Three-dimensional pulse compression for infrared nondestructive testing," IEEE Sensors Journal, 9(7), 832-833 (2009).

[16] Tabatabaei, N. and Mandelis, A., "Thermal-wave radar: A novel subsurface imaging modality with extended depth-resolution dynamic range," Review of Scientific Instruments, 80(3), 034902 (2009).

[17] Ghali, V.S., Mulaveesala, R. and Takei, M., "Frequency-modulated thermal wave imaging for non-destructive testing of carbon fiber-reinforced plastic materials, "Measurement Science and Technology, 22(10), 104018 (2011).

[18] Ghali, V.S., Panda, S.S.B. and Mulaveesala, R., "Barker coded thermal wave imaging for defect detection in carbon fbre-reinforced plastics," Insight: Non-Destructive Testing and Condition Monitoring, 53(11), 621-624 (2011).

[19] Mulaveesala, R., and Ghali, V. S., "Coded excitation for infrared non-destructive testing of carbon fiber reinforced plastics," Review of Scientific Instruments, 82(5), 054902 (2011).

[20] Tabatabaei, N., Mandelis, A. and Amaechi, B. T., "Thermophotonic radar imaging: An emissivity-normalized modality with advantages over phase lock-in thermography," Applied Physics Letters, 98(16), 163706 (2011).

[21] Ghali, V. S. and Mulaveesala, R., "Comparative data processing approaches for thermal wave imaging techniques for non-destructive testing," Sensing and Imaging, 12, 15-33 (2011).

[22] Tabatabaei, N., Mandelis, A. and Amaechi, B. T., "Thermophotonic radar imaging: An emissivity-normalized modality with advantages over phase lock-in thermography," Applied Physics Letters, 98(16), 163706 (2011).

[23] Ghali, V. S. and Mulaveesala, R., "Quadratic frequency modulated thermal wave imaging for non-destructive testing," Progress In Electromagnetics Research M, 26, 11-22 (2012).

[24] Mulaveesala, R., Ghali, V. S. and Arora, V., "Applications of non-stationary thermal wave imaging methods for characterisation of fibre-reinforced plastic materials," Electronics Letters, 49(2), 118-119 (2013).

[25] Dua, G. and Mulaveesala, R., " Applications of Barker coded infrared imaging method for characterisation of glass fibre reinforced plastic materials," Electronics Letters., 49 (17), 1071-1073 (2013).

[26] Mulaveesala, R., Ghali, V. S. and Arora, V., "Applications of non-stationary thermal wave imaging methods for characterisation of fibre-reinforced plastic materials," Electronics Letters, 49(2), 118-119 (2013).

[27] Arora, V. and Mulaveesala, R., "Pulse compression with Gaussian weighted chirp modulated excitation for infrared thermal wave imaging," Progress in Electromagnetics Research Letters, 44, 133-137 (2014).

[28] Arora, V., Siddiqui, J.A., Mulaveesala, R., and Muniyappa, A. " Pulse compression approach to nonstationary infrared thermal wave imaging for nondestructive testing of carbon fiber reinforced polymers," IEEE Sensors Journal, 15 (2), 6936841, 663-664 (2015).

[29] Arora, V., Mulaveesala, R., Siddiqui, J.A., and Muniyappa, A." Hilbert transform-based pulse compression approach to infrared thermal wave imaging for sub-surface defect detection in steel material," Insight: Non-Destructive Testing and Condition Monitoring, 56 (10), 550-552 (2015).

[30] Dua, G., Mulaveesala, R., and Siddiqui, J.A., " Effect of spectral shaping on defect detection in frequency modulated thermal wave imaging," Journal of Optics., 17 (2), 025604 (2015).